



DERIVATION OF ATTENUATION RELATIONS OF ARIAS INTENSITY USING THE CHI-CHI EARTHQUAKE DATA

Howard HWANG¹, Chih-Kun LIN² and Yeong-Tein YEH³

SUMMARY

This paper presents a derivation of attenuation relations of Arias intensity for various site conditions based on the strong-motion data recorded in the 1999 Chi-Chi Taiwan earthquake. The data are from the mainshock and three large aftershocks with stations in the footwall area and in the area away from the fault. At each station, Arias intensity is computed from two horizontal acceleration time histories. The Arias intensity data are separated into four groups according to site classes B, C, D and E assigned to recording stations. For each site class, the attenuation relation of Arias intensity is derived using a two-step regression analysis method. The attenuation curves of Arias intensity for soil sites (site classes C, D, and E) have a similar shape. The attenuation curve for site class E has the largest amplitude and the attenuation curve for site class C has the smallest amplitude. In addition, the attenuation curve of Arias intensity for rock sites (site class B) decreases faster than the curves for soil sites (site classes C, D, and E). The attenuation relations established in this study can be used to estimate Arias intensity from a rupture of a thrust fault for sites in the footwall area or in the area away from the fault.

INTRODUCTION

During an earthquake, ground shaking is recorded at strong-motion stations. The recorded ground motion is affected by many factors, such as the characteristics of seismic source, the attenuation of seismic waves from the seismic source to a recording site, and the soil condition at the recording site. For engineering applications, ground shaking is usually described in terms of amplitude, frequency content, and duration of ground motion. Several parameters have been proposed as a measure of ground shaking. These parameters include peak ground acceleration, spectral acceleration, and Arias intensity.

Peak ground acceleration has been widely used to describe ground shaking. It provides a measure of the largest amplitude of ground motion, but it contains no information on the frequency content and duration of ground motion. Spectral acceleration is the maximum value of response acceleration of a single-degree-

¹ Professor, National I-Lan University, I-Lan, Taiwan. Email: hwanghmh@yahoo.com

² Engineer, CTCI Corporation, Taipei, Taiwan. Email: ctci52575@ctci.com.tw

³ Dean, Ching Yun University, Jung-Li, Taiwan, Email: ytyeh@mail.cyu.edu.tw

of-freedom (SDOF) system subject to an input ground motion. It is a function of the natural frequency and damping ratio of the SDOF system. It provides some information on the amplitude and frequency content of ground motion, but it does not contain any information on the duration of ground motion. Strictly speaking, spectral acceleration is not a parameter for describing ground motion; rather, it is a parameter for describing structural response to an earthquake. Arias intensity [1] is derived from the integration of the square of the entire acceleration time history; thus, Arias intensity includes the characteristics of amplitude, frequency content, and duration of ground motion. In recent years, Arias intensity has increasingly been used as a parameter for describing ground shaking by many researchers, for example, Kayen and Mitchell [2], Toprak [3], and Hwang et al. [4].

On September 21, 1999, a powerful earthquake of moment magnitude 7.7 occurred near the town of Chi-Chi in central Taiwan, resulting from a rupture of the Chelungpu fault, which is an east dipping thrust fault [5]. The Chi-Chi earthquake was followed by a very energetic aftershock sequence with more than 10,000 earthquakes recorded within a one-year period. Since 1991, the Central Weather Bureau (CWB) of Taiwan has installed about 700 free-field strong-motion stations on the island of Taiwan [6]. With this extensive instrumentation, strong-motion data resulting from the mainshock and aftershocks of the Chi-Chi earthquake are well recorded.

The objective of this study is to develop attenuation relations of Arias intensity for various site conditions based on the strong-motion data recorded in the Chi-Chi earthquake. The data used in this study are from the mainshock and three large aftershocks with recording stations located in the footwall area and in the area away from the fault. At each station, Arias intensity is computed from two horizontal acceleration time histories. The site conditions of recording stations are classified into four site classes and the Arias intensity data are separated into four groups accordingly. For each site class, the attenuation relation of Arias intensity is expressed as a function of moment magnitude and source distance and it is derived using a two-step regression analysis method proposed by Joyner and Boore [7, 8]. The attenuation relations established in this study can be used to estimate Arias intensity from a rupture of a thrust fault for sites located in the footwall area or in the area away from a fault.

TAIWAN STRONG-MOTION SEISMIC NETWORK

Since 1971, the Central Weather Bureau of Taiwan has initiated a program to install strong-motion instruments on the island of Taiwan. The Taiwan strong-motion seismic network consists of about 700 free-field strong-motion stations as shown in Figure 1. Each station includes triaxial accelerometers, a digital recorder, a power supply, and a GPS timing system. Most of the digital accelerometers used in these stations are ± 2 g full scale, 200 or higher samples per second, and 16-bit or better resolution with up to 20-second pre-event recording. Only one type of older digital accelerometer, A800, has a 12-bit resolution [6]. The strong-motion stations are spaced approximately 5 km apart in nine metropolitan regions.

The strong-motion stations are located in various site conditions. Lee et al. [9] performed a site classification for 708 free-field stations of the Taiwan strong-motion network. They classified the sites of strong-motion stations into four site classes, B, C, D, and E. It is noted that the site classes defined by Lee et al. are compatible with those specified in the NEHRP provisions [9]. Generally speaking, site class B is rock sites, site class C is sites with very dense soils, site class D is sites with stiff soils, and site class E is sites with soft soils. The site classes established by Lee et al. for all strong-motion stations are utilized in this study.

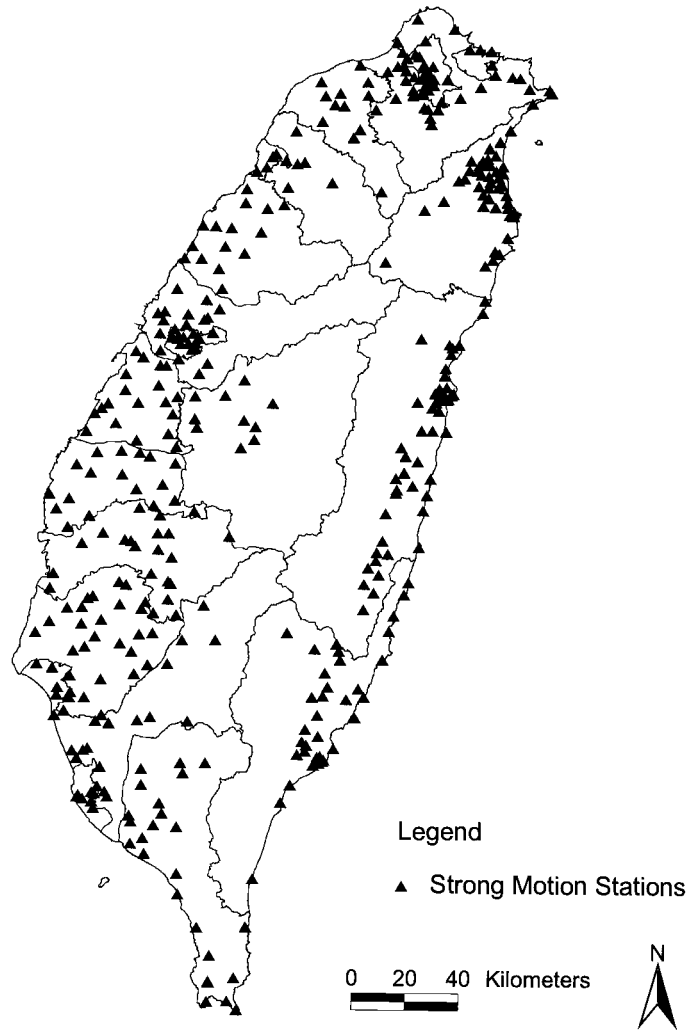


Figure 1. Free-field strong-motion stations on the island of Taiwan.

STRONG MOTION DATA

After the Chi-Chi earthquake, approximately 100 km of the surface trace of the ruptured Chelungpu fault were mapped in detail by the Central Geological Survey (CGS) of Taiwan. The result was published in a series of 1:25,000 scale maps [10]. Based on these maps, a digital coverage of the Chelungpu fault (Figure 2) is created using ArcView, a geographic information system (GIS) software package [11]. The shortest horizontal distance from a recording station to the surface projection of a fault rupture plane is denoted as R . Since the ruptured Chelungpu fault has a surface trace, this surface trace is considered as the surface projection of the fault. The shortest horizontal distances R of all strong-motion stations to the surface trace of the ruptured Chelungpu fault are determined using the spatial analysis tools built into ArcView. As an illustration, the shortest horizontal distance from station TCU055 to the surface trace of the Chelungpu fault is shown in Figure 2. The source distance r is defined as follows:

$$r = (R^2 + h^2)^{1/2} \quad (1)$$

where R is the shortest horizontal distance from a station to the surface projection of a fault in km and h is the focal depth in km.

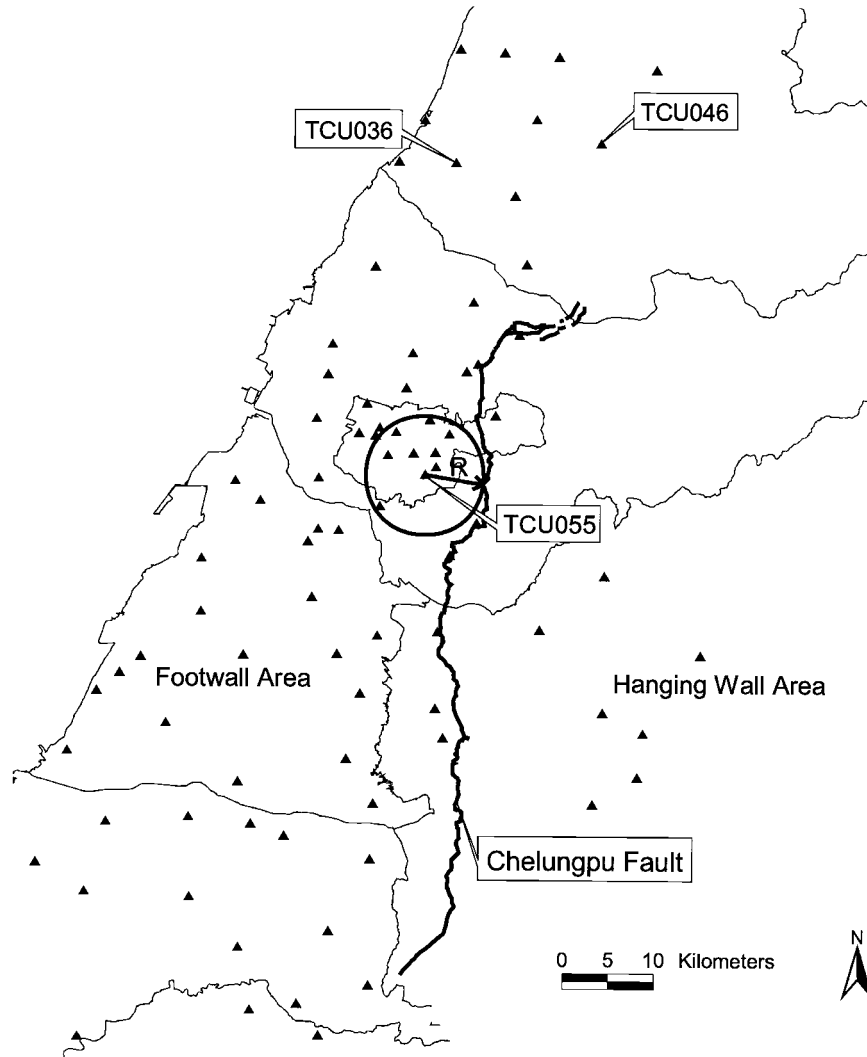


Figure 2. Strong-motion stations around the Chelungpu fault.

The strong-motion data used in this study are from the mainshock and three large aftershocks of the Chi-Chi earthquake with the baseline correction performed by Dr. Yeong-Tein Yeh and his associates [12]. As shown in Table 1, the mainshock is denoted as event 1, and three aftershocks are denoted as events 2, 3, and 4, respectively. The moment magnitudes M_w , and focal depths of these four events are also listed in Table 1 [12, 13].

Table 1. Summary of four earthquake events

Event	Mainshock / aftershock	Date	Universal time	Focal depth (km)	Moment magnitude M_w
1	Mainshock	1999/09/20	17:47:15.85	8.0	7.7
2	Aftershock	1999/09/20	18:03:40.83	3.5	6.2
3	Aftershock	1999/09/22	00:14:40.77	15.6	6.4
4	Aftershock	1999/09/25	23:52:49.51	9.9	6.5

The criteria for selecting strong-motion data for this study are as follows:

1. The A800 accelerometer has a 12-bit resolution, which is less than the resolution of other accelerometers installed in the Taiwan strong-motion seismic network. Furthermore, the stations with A800 accelerometers are collocated at the stations with A900 or A900A accelerometers. Thus, the strong-motion data recorded at 37 stations with A800 accelerometers are excluded.
2. The high peak horizontal acceleration recorded at station TCU129 is due to the effects of a concrete recording pier [14]. Thus, the strong-motion data recorded at TCU129 are excluded.
3. The site classes of 7 strong-motion stations are not available. The strong-motion data recorded at these stations are excluded.
4. The characteristics of strong motions in the hanging wall area are quite different from those in the footwall area [15]. The data used in this study are from stations located in the footwall area; thus the strong-motion data recorded at 13 stations located in the hanging wall area are excluded.

Since local site conditions have significant effects on ground shaking, the strong-motion data are separated into four groups according to site classes B, C, D, and E assigned to recording stations. The numbers of strong-motion data in each site class are shown in Table 2.

Table 2. Numbers of strong-motion data corresponding to four site classes

Event	Number of selected data	Site class B	Site class C	Site class D	Site class E
1	387	48	62	177	100
2	316	24	50	151	91
3	367	45	53	170	99
4	356	38	56	166	96
Total	1426	155	221	664	386

ESTIMATION OF ARIAS INTENSITY

Arias intensity I_h is the total energy per unit weight stored in a set of undamped linear oscillators at the end of an earthquake. By Parseval's theorem, it can be shown that Arias intensity has a close relation with the area under the square of the amplitude of the Fourier amplitude spectrum computed from the acceleration time history [1]. The Arias intensity for ground acceleration in the east-west direction is determined as follows:

$$I_{EW} = \frac{\pi}{2g} \int_0^{t_0} [a_{EW}(t)]^2 dt \quad (2)$$

where I_{EW} is the Arias intensity in the east-west direction, $a_{EW}(t)$ is the acceleration time history in the east-west direction, and t_0 is the total duration of ground motion. The Arias intensity in the north-south direction I_{NS} can be determined in the same way. Because of the additive nature of scalar energy measures, Arias intensity I_h is defined as the sum of these two horizontal Arias intensities.

$$I_h = I_{EW} + I_{NS} \quad (3)$$

where I_h is expressed in the unit of m/sec. The Arias intensity values at all the strong-motion stations from four earthquakes are determined and the results are shown in a report by Hwang et al. [15].

TWO-STEP REGRESSION ANALYSIS

Arias intensity is affected by many factors, such as the characteristics of the seismic source, the attenuation of seismic waves from a seismic source to a recording site, and the soil condition at a recording site. In this study, the characteristics of seismic source are represented by the moment magnitude M_w , the path attenuation is represented by the source distance or the shortest horizontal distance, and the site conditions at recording stations are represented by four site classes. In this study, the Arias intensity data are classified into four groups according to four site classes B, C, D, and E assigned to recording stations. For each site class, the regression model for Arias intensity is as follows:

$$\ln I_h = a M_w + b \ln r + c + \varepsilon \quad (4)$$

where I_h is Arias intensity in m/sec, M_w is the moment magnitude, r is the source distance in km, and ε is the random error, which follows a normal distribution with zero mean and variance σ^2 . The coefficients a , b , and c are unknown regression coefficients.

In general, the data used in the regression analysis include data recorded at many strong-motion stations in several earthquakes. If a regression analysis is performed to determine coefficients for magnitude and distance simultaneously, errors in measuring magnitude may affect the distance coefficient obtained from the regression analysis [7, 16]. To avoid this interaction, Joyner and Boore [7] proposed a two-step regression analysis method. In the first step, the distance coefficient is determined along with a set of amplitude factors, one for each earthquake. In the second step, the amplitude factors are regressed to determine the magnitude coefficient. The advantage of this approach is that it decouples the determination of the magnitude dependence from the determination of the distance dependence. In this study, the two-

step regression analysis method as proposed by Joyner and Boore [7, 8] is used to derive the attenuation relation of Arias intensity. The detail is shown in a report by Hwang et al. [15].

RESULTS AND DISCUSSION

As shown in Table 2, the numbers of data with site classes B, C, D, and E are 155, 221, 664, and 386, respectively. Using the Arias intensity data for each site class, a two-step regression analysis is performed to derive the attenuation relation of Arias intensity for that site class. The regression results are summarized in Table 3. As an illustration, the median, 84th, and 16th percentile curves of Arias intensity for site class D, moment magnitude 7.7, and focal depth 8 km are shown in Figure 3. The Arias intensity data from the mainshock (event 1) are also plotted in the figure. As shown in the figure, most of the Arias intensity data fit very well between the 84th and 16th percentile attenuation curves.

Table 3. Regression results from two-step regression analysis method

Site class	Regression coefficients			
	a	b	c	σ
B	2.071	-2.178	-8.492	1.29
C	2.290	-1.245	-13.539	1.23
D	2.155	-1.323	-11.920	1.25
E	1.746	-1.585	-7.409	0.82

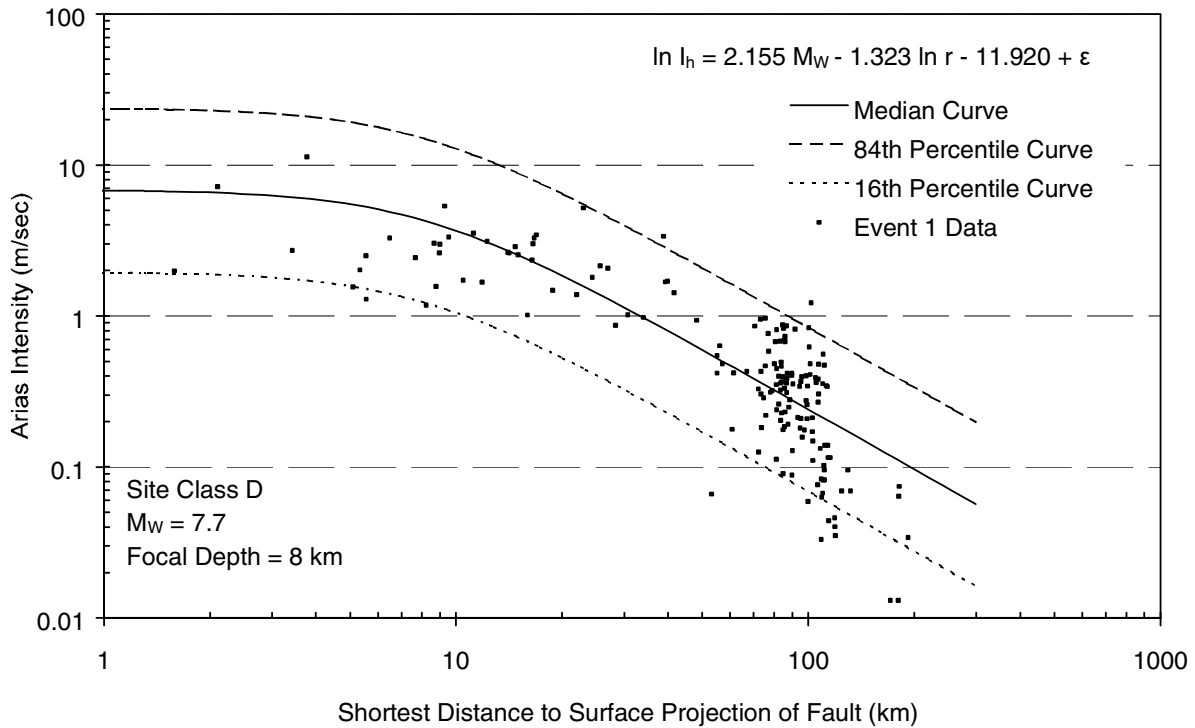


Figure 3. Attenuation curves of Arias intensity for site class D.

The median attenuation curves of Arias intensity for site class D, focal depth 10 km, and four moment magnitudes 7.5, 7.0, 6.5, and 6.0 are shown in Figure 4. As expected, the amplitude of the attenuation curve resulting from an earthquake with large moment magnitude is higher than that resulting from an earthquake with small moment magnitude.

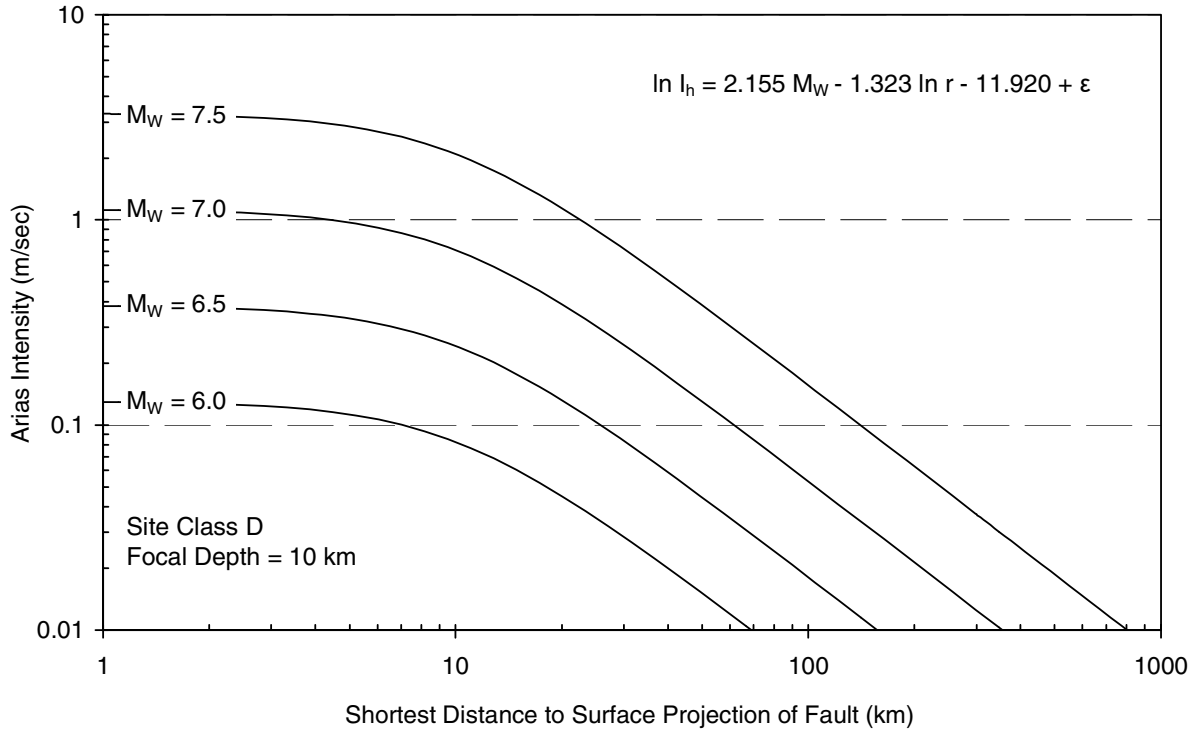


Figure 4. Median attenuation curves of Arias intensity with four moment magnitudes.

For moment magnitude 7.0 and focal depth 10 km, the median attenuation curves of Arias intensity for four site classes B, C, D, and E are shown in Figure 5. It is noted that site class B is rock sites, site class C is sites with very dense soils, site class D is sites with stiff soils, and site class E is sites with soft soils. As shown in Figure 5 the attenuation curves for soil sites (site classes C, D, and E) have a similar shape. The attenuation curve for site class E has the largest amplitude and the attenuation curve for site class C has the smallest amplitude. The results are expected, since ground motions are amplified when seismic waves travel through soils; the sites with soft soils (site class E) usually exhibit larger amplification than the sites with very dense soils (site class C). Also shown in Figure 5, the attenuation curve of Arias intensity for rock sites (site class B) decreases faster than the curves for soil sites (site classes C, D, and E). This is due to the fact that the seismic waves are reflected and refracted within soil layers; thus the energy carried by seismic waves travels farther away from the seismic source and the bracketed duration of strong ground motion is longer at soil sites than at rock sites. As a result, the attenuation curve of Arias intensity for rock sites has a steeper slope than the attenuation curves for soil sites.

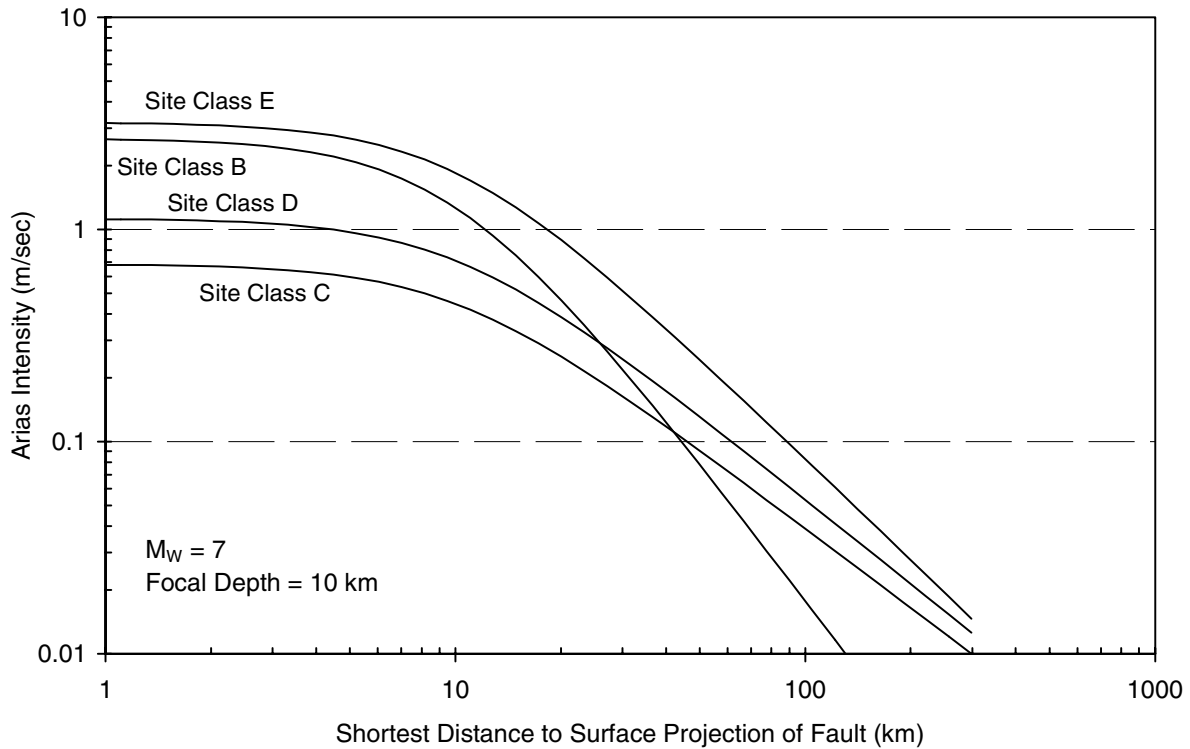


Figure 5. Comparison of median attenuation curves of Arias intensity for four site classes.

CONCLUSIONS

The attenuation relations of Arias intensity for four site conditions have been developed based on the Chi-Chi Taiwan earthquake data. The attenuation curves of Arias intensity for soil sites (site classes C, D, and E) have a similar shape. The attenuation curve for site class E has the largest amplitude and the attenuation curve for site class C has the smallest amplitude. In addition, the attenuation curve of Arias intensity for rock sites (site class B) decreases faster than the curves for soil sites (site classes C, D, and E). The attenuation relations of Arias intensity for four site classes established in this study can be used to estimate Arias intensity from a rupture of a thrust fault for sites located in the footwall area or in the area away from the fault.

ACKNOWLEDGMENTS

This paper is based on research partially supported by the National Science Council of Taiwan under Grant NSC91-2625-Z-231-001-(Yeong Tein Yeh). We are indebted to the staff members and advisors of the Seismology Center of the Central Weather Bureau of Taiwan for their dedication in operation of strong-motion seismic network.

REFERENCES

1. Arias A. "A measure of earthquake intensity." Hansen RJ, Editor. Seismic Design for Nuclear Power Plants. Cambridge: The M.I.T. Press, 1970: 438-489.

2. Kayen RE, Mitchell JK. "Assessment of liquefaction potential during earthquake by Arias intensity." *Journal of Geotechnical and Geoenvironmental Engineering* 1997; 123(12): 1162-1174.
3. Toprak S. "Earthquake effects on buried lifeline systems." PhD Dissertation, Ithaca: Cornell University, 1998.
4. Hwang H, Chiu YH, Chen WY, Chen YC, Shih BJ, Liu PS. "Damage analysis of Taichung gas pipelines resulting from the Chi-Chi Taiwan earthquake." Technical report, Center for Earthquake Research and Information, Memphis: The University of Memphis, 2002.
5. Shin TC, Teng TL. "An overview of the 1999 Chi-Chi, Taiwan, earthquake." *Bulletin of the Seismological Society of America* 2001; 91(5): 895-913.
6. Liu KS, Shin TC, Tsai YB. "A free-field strong motion network in Taiwan: TSMIP." *Journal of Terrestrial, Atmospheric and Oceanic Sciences* 1999; 10(2): 377-396.
7. Joyner WB, Boore DM. "Peak horizontal acceleration and velocity from strong-motion records including records from the 1979 Imperial Valley, California, earthquake." *Bulletin of the Seismological Society of America* 1981; 71(6): 2011-2038.
8. Joyner WB, Boore DM. "Methods for regression analysis of strong-motion data." *Bulletin of the Seismological Society of America* 1993; 83(2): 469-487.
9. Lee CT, Cheng CT, Liao CW, Tsai YB. "Site classification of Taiwan free-field strong-motion stations." *Bulletin of the Seismological Society of America* 2001; 91(5): 1283-1297.
10. Central Geological Survey (CGS). "Surface Ruptures Along the Chelungpu Fault During the Chi-Chi Earthquake, Taiwan." Taipei: Ministry of Economic Affairs, 1999.
11. Environmental Systems Research Institute (ESRI). "Using ArcView GIS." Redlands: Environmental Systems Research Institute, 1996.
12. Cheng SN, Yeh YT, Loh CH, Chang CH, Shin TC. "Strong-motion data reduction for aftershocks of Chi-Chi earthquake." *Proceedings of International Workshop on Annual Commemoration of Chi-Chi Earthquake*. Taipei: National Center for Research on Earthquake Engineering, 2000: 275-282.
13. Chen KC, Huang BS, Wang JH, Yeh HY. "Conjugate thrust faulting associated with the 1999 Chi-Chi, Taiwan, earthquake sequence." *Geophysical Research Letters* 2002; 29(8): 1181-1184.
14. Wen KL, Peng HY, Tsai YB, and Chen KC. "Why 1G was recorded at TCU129 site during the 1999 Chi-Chi, Taiwan, earthquake." *Bulletin of the Seismological Society of America* 2001; 91(5): 1255-1266.
15. Hwang H, Lin CK, Yeh YT, Cheng SN, Chen KC. "Attenuation relationship of Arias intensity based on the Chi-Chi Taiwan earthquake data." Technical report, Center for Earthquake Research and Information, Memphis: The University of Memphis, 2003.
16. Fukushima Y, Tanaka T. "A new attenuation relation for peak horizontal acceleration of strong earthquake ground motion in Japan." *Bulletin of the Seismological Society of America* 1990; 80(4): 757-783.